The historical climate trend resulted in changed ~~convective~~ vertical transport patterns in climate model simulations

Adrienne Jeske[1] and Holger Tost[1]

[1]Institute for Atmospheric Physics, Johannes Gutenberg-University Mainz, Mainz, Germany

Correspondence: Adrienne Jeske (adjeske@uni-mainz.de)

Abstract. Convective transport leads to a rapid vertical redistribution of tracers. This has a major influence on the composition of the upper troposphere, a highly ~~climate sensitive~~ climate-sensitive region. It is not yet clear how the convective transport is affected by climate change. In this study, we applied a new tool, the so-called convective exchange matrix, in historical simulations with the chemistry-climate model EMAC (ECHAM/MESSy Atmospheric Chemistry) ~~chemistry-climate model~~ to investigate the trends in convective transport. The simulated deep convection is penetrating higher, but occurs less frequently from 2011 to 2020 than from 1980 to 1989. The increase in the vertical ~~extend~~ extent of convection is highly correlated ~~to~~ with a rise in the tropopause height. ~~Overall, convection transports material less efficient~~ The upward transport increased on average to height levels of 130 hPa and above, but convection transported material less efficiently to the upper troposphere ~~, but the transport directly into the tropopause region has on average increased~~ in general from 2011 to 2020 in comparison to the ~~1980ies~~1980s. These findings give rise ~~for~~ to new opportunities to investigate ~~long term~~ long-term simulations performed by EMAC with regard to the effects of convective transport. ~~Further~~Furthermore, they might provide a first insight into the trends of atmospheric convective transport due to changing atmospheric conditions and might serve as an estimate for the convective feedback to climate change.

1 Introduction

Moist convection plays a key role for the transport of heat and water in the Earth's atmosphere (**?**). Beyond that, deep convection is associated with extremely large vertical wind velocities. These lead to ~~rapid~~ short vertical transport time scales and ~~therefore, to a major~~ to a rapid redistribution of atmospheric tracers (**?**). Consequently, convective transport has complex implications for the atmospheric composition and chemistry, especially in the upper troposphere (**???**). As some studies argue, deep convection even influences the composition of the lower stratosphere (**???**) and could lead to a downward transport of ~~ozone rich~~ ozone-rich air from the stratosphere to the upper troposphere (**?**).

Because it is highly important to capture convective transport and its effects (**?**), many efforts were made towards a better representation of convective transport in models (**????**), a more comprehensive understanding of this process (**???**), and the interplay of convective transport and the related scavenging ~~(?????). However it is not known yet, how convective transport will adapt to climate change.~~ of tracers (**?????**).

~~Despite the transport effects, it is a hot topic in literature, how convection has changed and will change due to the extensive changes in our climate system we are facing~~Global warming affects atmospheric convection and might also influence convective transport. **?** found with the help of CMIP6 (Coupled Model Intercomparison Project Phase 6, **?**) simulation data that ~~in a warmer climate~~ CAPE (convective available potential energy) increases in a warmer climate, likely causing an enhancement in severe storm frequency. ~~**?** performed simulations with doubled CO2 concentrations and~~ **?** examined the changes in the ice water path in convective clouds due to temperature and CO_2 changes. The observed changes were closely linked to changes of the vertical upward velocities within convective clouds (**?**). Already **?** detected an increase in the updraft velocity ~~in this case.~~ performing simulations with doubled CO_2 concentrations. The effect of warming on the updraft intensity was also confirmed by **?**.

~~If the~~ In case of a change of either convection occurrence or strength ~~of convection changes~~(or both), it can be assumed that the corresponding convective transport will be modified as well. **?** performed a ~~40 year~~ 40-year projection to investigate the trends of tropospheric ozone concentrations under climate warming conditions. ~~Thereby, is directly affected by convective transport itself and of its precursors as well as lightning emissions in deep convective cells (**?**).~~ Within this simulation, the tropical convection occurs less frequently in the 2020s compared to the 1990s, but the updrafts strengthened at about 150 hPa, which influences the vertical transport. ~~**?** found, that the changes in the convective properties lead to a decrease in the column ozone, what implies a negative chemistry-climate feedback according to the authors.~~

The work by **?** highlights the importance ~~to investigate~~ of investigating the adaptations of convective transport to understand the response of the climate system to warming. However, so far it is not fully clear ~~,~~ how convective transport processes change in detail and to ~~which~~ what extent. Therefore, ~~this~~ our study follows up with the question: How does climate change specifically ~~influences~~ influence the convective transport~~, i.e.,~~? How has the transport efficiency ~~by~~ and extent of the updraft, the downdraft~~and the large-scale subsidence and the vertical extend of these transport processes~~, and the balancing subsidence changed with time?

This manuscript addresses this question by performing historical simulations with the chemistry-climate model EMAC (ECHAM / MESSy Atmospheric Chemistry, **???**) using the convective transport scheme CVTRANS (ConVective tracer TRANSport) by **?**. To do so, we improved the representation of the turbulent detrainment and entrainment in CVTRANS and added a new feature to analyse convective transport, namely the convective exchange matrix ~~.~~ similar to the mixing matrix by **?**. This new tool connects ~~the~~ convective transport from all possible starting levels to all possible destination levels in a model when utilising a convection parameterisation. This enables a deeper understanding of the changing transport processes and their causes. The focus of this study lies on the changes in ~~the~~ deep convective transport towards the upper troposphere over the past decades.

This study is structured as follows: The global chemistry climate model EMAC and submodel CVTRANS are described briefly in Sec. 2. In the same section, we introduce the adaptations and added features within the new version of CVTRANS. The simulation setup is described in Sec. 2.4. In Sec. 3, we analyse the results, focusing on the changes in transport over the past decades. The implications, ~~significance~~ the significance, and the limitations are discussed in Sec. 4. The summary and the outlook are given in Sec. 5.

2 Model description

2.1 EMAC

The global chemistry and climate model EMAC (**???**) consists of the general circulation model ECHAM5 (European Centre Hamburg general circulation model version 5, **?**) and the Modular Earth Submodel System ~~(MESSy, ???)~~(MESSy, **????**). MESSy is ~~an interface~~ a software framework to couple different submodels with a chosen base model and includes a steadily growing number of these submodels. For example, **?** used EMAC recently to combine a global dynamic vegetation model with an atmospheric model. In this study, MESSy version 2.55 is used to link the submodel CVTRANS (**?**) with ECHAM. The dynamic representation of convection is given by the Tiedtke-Nordeng convection scheme (**??**), as implemented in the CONVECT submodel within the MESSy structure (**?**).

2.2 ~~Simulation setup~~

~~A three dimensional global simulation has been conducted with the convective exchange matrix implemented utilising the chemistry climate model EMAC (??). 31 vertical pressure level up to 10 Pa are used and a horizontal resolution of T63 (triangular truncation with wavenumber 63) has been applied. This is associated with 192 × 96 gridpoints and a time step of 12 min. The simulation period spans the time from the beginning of 1979 until the end of 2020.~~

~~Temperature, vorticity, divergence, surface pressure, sea surface temperature and sea ice consentrations are nudged towards ECMWF Reanalysis fifth generation (ERA5, ?). The nudging is based on ? and applied as described by ?. A basic methane chemistry is applied to take the water vapour production in the stratosphere and its influence on radiation into account using the submodel CH4 (?). Further considerations of chemical reactions are not necessary, because this study exclusively investigates the redistribution of air masses by convection and not the effect on single tracers. Monthly mean values for greenhouse gases are used to include their radiative effect based on ?. The ? climatology is used for tropospheric aerosol as described by ?. For the stratospheric aerosol radiative effect optical properties of the CCMI (Chemistry–Climate Model Initiative) database (?) are applied, e.g., as in ?.~~

~~The simulations have been performed at the national super computing system Mogon NHR (Nationales Hochleistunggsrechnen). The computing time tests have been conducted at Levante at the German Climate Computing Centre (DKRZ, Deutsches Klimarechenzentrum).~~

2.2 CVTRANS

The submodel CVTRANS (ConVective tracer TRANSport) was introduced by **?** to account for convective tracer transport in EMAC. This submodel can reproduce observed changes of the vertical profiles of non-soluble tracers due to convection sufficiently well (?). It makes use of a single plume/bulk ~~convection~~ convective transport parameterisation based on the formulation of ?. ? applied the convective mass fluxes for the updraft, downdraft, entrainment, and detrainment from the convection parameterisation to calculate the redistribution of the tracers. The mass fluxes must fulfil the following equations

$$F_{\mathrm{u}}^{k} = F_{\mathrm{u}}^{k+1} + E_{\mathrm{u}}^{k} + D_{\mathrm{u}}^{k} \tag{1a}$$

$$F_{\mathrm{d}}^{k+1} = F_{\mathrm{d}}^{k} + E_{\mathrm{d}}^{k} + D_{\mathrm{d}}^{k} \tag{1b}$$

as described by ? with F referring to the mass fluxes, D the detrainment and E the entrainment. The subscripts $_{\mathrm{u}}$ and $_{\mathrm{d}}$ denote the updraft and the downdraft. k indicates the model level. If this relation is not satisfied, the detrainment or entrainment should be adapted accordingly (?).

Strong updrafts can lead to mass balance problems, i.e., more mass is transported out of a model box as mass is transported into the box in one time step. The mass fluxes are ~~re-sealed~~ rescaled in such cases to prevent a mass imbalance. This procedure can lead to a damping of the convective transport. To overcome this issue, ? included intermediate time stepping in CVTRANS to ensure ~~an~~ optimum handling of ~~very strong~~ intense convective events.

Note ~~,~~ that the transport of water vapor and hydrometeors is not considered in the convective tracer transport algorithm, as the convection parameterisation itself takes care of the redistribution of water species.

2.3 Modifications of CVTRANS

2.3.1 Revision of the closure formulation in the CVTRANS submodule

Following ?, the detrainment and the entrainment are given by an organised and a turbulent driven component. This is equally valid for the downdraft and the updraft. In the Tiedtke-Nordeng scheme, the same approach is made (?).

In the former versions of CVTRANS by ? and ?, it could happen in some cases that the formulation of the closure eliminated the turbulent entrainment and detrainment~~due to turbulence~~. To ~~fulfill~~ fulfil Eq. 1, ~~the situation could arise~~ it could occur that the entrainment had to be set to zero to ~~calculate a closed mass balance; however~~close the mass balance. However, this would also erroneously eliminate the turbulent entrainment, which is always active in rapidly ascending or descending air masses. The entrainment rate is given by

$$E_{\mathrm{u}}^{k} = F_{\mathrm{u}}^{k} - F_{\mathrm{u}}^{k+1} + D_{\mathrm{u}}^{k}, \tag{2}$$

as long as the updraft mass flux leaving the box at its top is larger than the incoming updraft mass flux from below. All quantities are positive by definition.

If ~~instead~~ the incoming updraft mass flux is larger than the mass flux leaving the box at the top, the detrainment will be recalculated with the help of the closure as follows

$$D_{\mathrm{u}}^{k} = F_{\mathrm{u}}^{k+1} - F_{\mathrm{u}}^{k} + E_{\mathrm{u}}^{k}. \tag{3}$$

If both equations for entrainment and detrainment are properly solved, ~~no turbulent detainment or entertainment is~~ the detrainment or entrainment will not be accidentally set to zero. The same approach is taken for the downdraft.

~~A~~ The formulation following **?** for the turbulent mixing is embedded to ensure the existence of turbulent entrainment and detrainment in updrafts and downdrafts in the closure part, which corrects potentially erroneous zero turbulent events.

The adaptive time stepping by **?** must be applied~~, otherwise~~. Otherwise, the calculation of the air mass transport can lead to negative values or a ~~cutting~~ reduction of the strength of the mass fluxes. ~~Both consequences are not desirable. Hence, we argue that adaptive time stepping should be applied in every simulation using CVTRANS.~~

2.3.2 Detrainment of entrained air in the downdraft

In CVTRANS, the parameter f_{det} gives the portion of material that is detrained directly after the entrainment in the same box as described by **?**. f_{det} is only computed and applied for the calculations concerning the updraft detrainment. Taking turbulence into account, we need to adapt ~~equation~~ Eq. (2) from **?** also for the downdraft:

$$C_{\mathrm{d,det}}^{k} = \frac{(D_{\mathrm{d}}^{k} - f_{\mathrm{det}} E_{\mathrm{d}}^{k}) C_{\mathrm{d}}^{k} + f_{\mathrm{det}} E_{\mathrm{d}}^{k} C_{\mathrm{env}}^{k}}{D_{\mathrm{d}}^{k}}. \tag{4}$$

Thereby, C denotes the concentration of a tracer.

2.3.3 Description of the convective exchange matrix

? introduced the mixing matrix to show convective transport and mixing. The convective exchange matrix ~~builds upon the concept of CVTRANS~~makes use of the same basic principles as the mixing matrix by **?**. First, in every vertical model level $(1, 2, ..., N)$, one pseudo tracer $(\boldsymbol{P_1}, \boldsymbol{P_2}, ..., \boldsymbol{P_N})$ is initialised with a value of 1 kg m^{-2}. N denotes the number of model levels. An important remark: By definition, the vertical model level with the highest number, level N, is closest to the surface.

In all other levels, the pseudo tracers are set equal to zero. The vertical profiles of the pseudo tracers can be written as N~~dimensional~~ -dimensional vectors. Applying this, the pseudo tracer $\boldsymbol{P_1}$ is given by $\boldsymbol{P_1} = (1, 0, 0, ..., 0)$ and $\boldsymbol{P_2}$ is $\boldsymbol{P_2} = (0, 1, 0, ..., 0)$. Putting all these vectors together results in an $N \times N$ diagonal matrix, as can be seen on the left side of Fig. 1(a).

The time integration, i.e., the vertical redistribution by convective transport of the pseudo tracer field, is performed based on ~~CVTRANS. This~~ the transport routine in CVTRANS (compare **?**) for the convective exchange matrix. The considered processes are shown in Fig. 1(b). The time integration results in the convective exchange matrix (**TrMa**). The entries of the matrix give the portion of the air mass (m_{air}) that was transported from a specific level (given by the pseudo tracer field in the beginning) to a certain departure level. For example, $\mathbf{TrMa}_{i,j}$ with $i, j = 1, ..., N$ describes how much m_{air} was transported from level i to level j. ~~Is~~ If $j = i$, then $\mathbf{TrMa}_{i,i}$ ~~characterise~~ characterises the contribution of level i to level i itself. In other words, it shows the amount of air that was not affected during the convective event. This is illustrated in Fig. 1(~~b~~c) highlighted in red. The upper left entries (yellow in Fig. 1) represent the transport from a level i to level j with i > j, i.e., the upward transport to level j which started in level i. Thereby, the notation is that the lowest model level has the highest number and the uppermost level is level 1. The downward transport (transport from a lower level number to a higher level number in this notation) is marked by the blue colour in Fig. 1(~~b). The illustration~~ c).

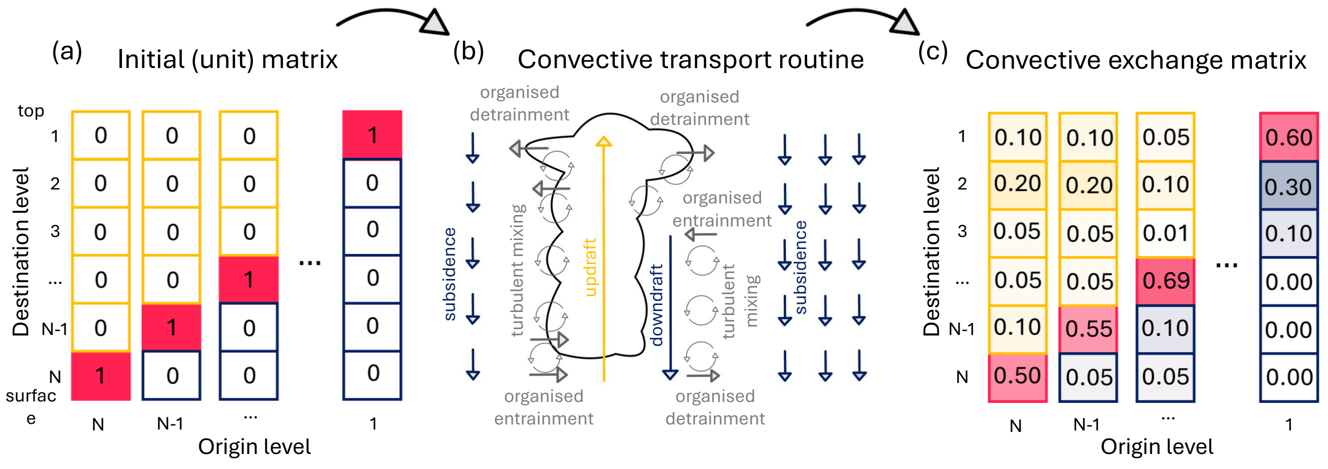

Figure 1. Sketch of the principle behind the convective exchange matrix. (a) shows the input matrix~~that is redistributed by~~. (b) illustrates the convective transport processes. The ~~redistribution is calculated with the submodule CVTRANS. The red arrows indicate~~ yellow arrow indicates the updraft~~mass flux~~, the blue ones the ~~organised detraning~~ downdraft and ~~entraining~~ the mass-balancing subsidence and the ~~thin black~~ grey ones the organised and turbulent ~~mixing~~detrainment and entrainment. The ~~convective exchange matrix~~ redistribution is ~~a result of~~ calculated with the ~~interplay of updraft, downdraft, large-scale subsidence, entrainment and detrainment from/into up- and downdraft, but, for simplicity, only~~ transport routine within the ~~updraft related processes are shown in this sketch~~submodule CVTRANS. Panel (~~b~~c) shows an example of a convective exchange matrix. (~~b~~c) is only for illustration and not a ~~real~~ case calculated during a simulation. In both matrices, the reddish coloured fields denote the main diagonal. The yellow fields ~~shows~~ show the matrix entries influenced by the updraft and the blue fields denote the matrix entries affected by the downdraft and the ~~large-scale~~ grid-scale subsidence. Synoptic-scale processes are not considered.

Figure 2 shows how the convective transport matrix is structured (a) in the tropics and (b) in the mid-latitudes. The highest model level number (31) refers to the level closest to the surface / the level with the highest pressure. This is the case for the destination and origin levels.

In Figure 2, the red diagonal is located where the origin level is equal to the destination level. This diagonal provides information about the air mass which stays at the same level, or in other words, is not affected by the convection. Roughly the following characteristics of convective upward motion (yellow in Fig. ~~S1 in the electronically supplements can be used as guideline for the interpretation of the~~ 2) are visible in the convective exchange matrix: (1) Shallow convection and turbulent detainment, when the origin level is located in the boundary layer and the destination level is as well in the boundary layer or in the lower troposphere, (2) deep convective updrafts reach up to the upper troposphere originating in the boundary layer, (3) some deep convective events reach even the height of the tropopause and beyond (left upper corner in Fig. 2(a) and (b), (4) upward transport starts also in free tropospheric levels and in upper tropospheric levels mainly due to turbulent entrainment into the updrafts. The downward motion is shown in blue in Fig. 2. The mass balancing subsidence is especially visible in the adjacent diagonals below the main diagonal. The subsidence can reach further towards lower pressure, the stronger the convective event is. The outflow of the downdraft is located in the boundary layer levels.

The difference between the tropics and the mid-latitudes is that the convective exchange matrix is compressed in the mid-latitudes, figuratively speaking (compare Fig. 2(a) and (b)). The tropopause is located at higher pressures (higher model level numbers) in the mid-latitudes compared to tropical regions.

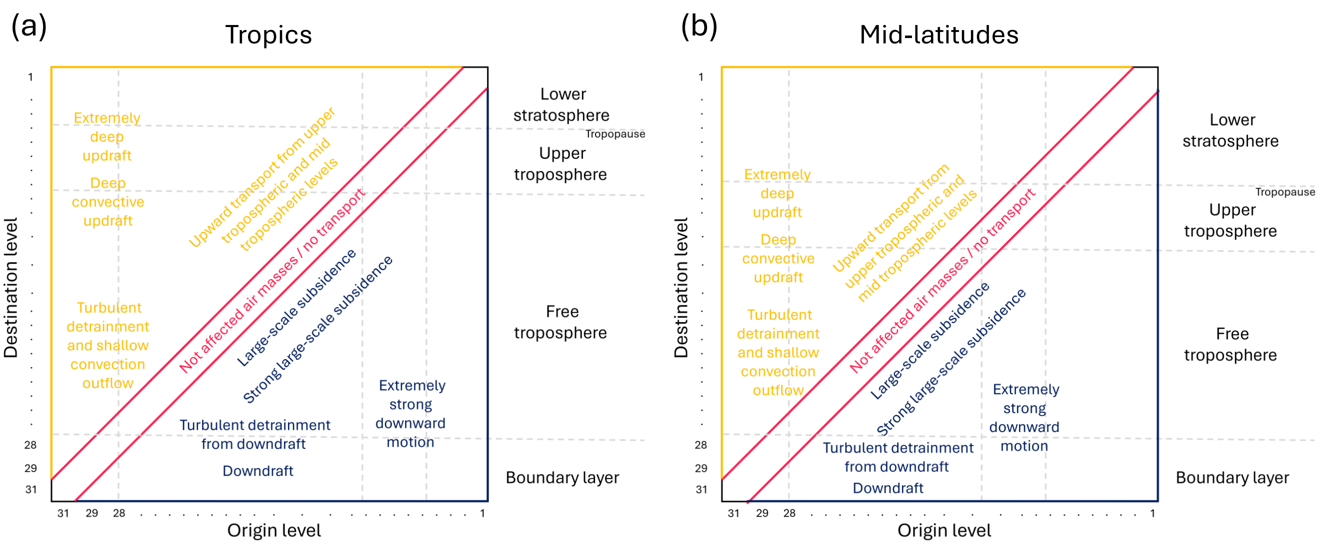

Figure 2. The convective exchange matrix is illustrated, including areas with roughly reflect specific transport mechanisms. This sketch can be used as an interpretation assistance of the convective exchange matrix. (a) shows the convective exchange matrix with regard to the tropics and (b) with regard to the mid-latitudes. The colour code is as in Fig. 1.

The redistributed concentrations of trace species can be calculated with the convective exchange matrix by a simple matrix multiplication of the TrMa with the vertical tracer mixing ratio profile, as now implemented in CVTRANS v3.0. For a ~~small~~ large number of tracers (∼ 100 tracers), the computational efficiency is similar when the convective exchange matrix is applied to calculate the new concentrations of the tracers after the convective transport instead of using the transport algorithm itself. Consequently, for a higher number of tracers, this new algorithm can become computationally more efficient.

The advantage of the convective exchange matrix is that the effects of the tracer transport can be studied disentangled from the specific background profiles of the tracers. Thus, it can be investigated, e.g., where the maximum outflow height is located and how much air mass can be transported upward inside ~~the undiluted core of the convective system~~a whole model grid cell. The contribution to a certain destination level can also be calculated for all starting levels. This can be helpful to track a measured air mass containing tracers backward and to investigate how strongly it was affected by convection in its air mass history.

2.4 Simulation setup

Three-dimensional global simulations have been conducted with the convective exchange matrix implemented utilising EMAC. 31 vertical pressure levels up to 10 hPa are used and a horizontal resolution of T63 (triangular truncation with wavenumber 63) has been applied. This is associated with 192 × 96 grid points with areas between 32.5 km × 32.5 km in the polar regions and 207.9 km × 207.9 km in the tropics and a time step of 12 min.

Temperature, vorticity, divergence, and surface pressure are nudged towards ECMWF Reanalysis fifth generation (ERA5, **?**) and the sea surface temperature and the sea ice coverage are prescribed by the nudging data. The nudging is based on **?** and applied as described by **?**.

The essential submodels for this study are mentioned in the following. An overview of the used submodels is given in the supplements (Table S1). A basic methane chemistry is applied to take the water vapour production in the stratosphere and its influence on radiation into account using the submodel CH4 (**?**). Further considerations of chemical reactions are not necessary, because this study exclusively investigates the redistribution of air masses by convection and not the effect on single tracers. Monthly mean values for greenhouse gases are used to include their radiative effect based on **?**. The **?** climatology is used for tropospheric aerosol as described by **?**. For the stratospheric aerosol radiative effect, optical properties of the CCMI (Chemistry–Climate Model Initiative) database (**?**) are applied, e.g., as in **?**.

The submodel CONVECT by (**?**) is applied with the Tiedtke-Nordeng scheme to calculate the parametrised convective properties needed in CVTRANS to calculate the convective exchange matrix. Three simulations were performed with slightly different CVTRANS versions: (1) One with the old version of CVTRANS but including the Convective Exchange Matrix (CVTRANSold), (2) one with CVTRANS 3.0 and enhanced turbulent mixing (CVTRANSturb), and (3) one with the standard CVTRANS 3.0. (CVTRANSnew). (1) and (2) are only used to show the impact the turbulent mixing has on the transport by one deep convective event. Therefore, only a short simulation period is chosen. The simulation period of (3) spans the time from the beginning of 1979 until the end of 2020, because (3) is used to study the climate impact on the convective transport in this study.

Table 1. Three global simulations were performed with different setups to test the effect of turbulent mixing on the convective transport. The simulations only vary in the used version and configuration of CVTRANS, as listed above, and in the simulation time.

Name	Version	Turbulence adjustment	Used in Section
CVTRANSold	v2	no adjustment	3.1
CVTRANSturb	v3	strong turbulence	3.1
CVTRANSnew	v3	weak turbulence	3.1 & 3.2

3 Results

In this section, the differences in the convective exchange matrix are investigated due to the adaptations in CVTRANS based on one example case. Afterwards, the convective exchange matrix is applied to study the effect of climate change on the convective transport. For the latter case, nudged historical simulations were performed.

3.1 Intercomparison of the adaptations using the convective exchange matrix

We performed three global simulations to demonstrate the effects of the described changes in the submodel CVTRANS (Table 1). One simulation was ~~made~~ derived for comparison applying the former default version of CVTRANS (CVTRANSold). The second was performed with CVTRANS modified as described in ~~the~~ Sec. 2.3.1 and 2.3.2 (CVTRANSnew). ~~A second was derived for comparison applying the former default version of CVTRANS (CVTRANSold).~~ The last one is similar to CVTRANSnew but with enhanced turbulent mixing (CVTRANSturb). Despite the Convective exchange matrix is a new feature in CVTRANS 3.0, this tool was implemented and turned on in all simulations. Thus, the convective exchange matrices can be compared for the different treatments of turbulent mixing.

Figure 3(a) shows the convective exchange matrix derived with CVTRANSold for one exemplary deep convective event. ~~The convective transport does not influence a large portion of the air mass in many levels. This can be clearly seen on the main diagonal of the convective exchange matrix.~~ The portion of air mass that stays in the ~~same~~ origin level ranges between 6.96 % and 92.43 % for all levels where convection is active ~~. The large-scale~~ (see main diagonal in Fig. 3(a)). The convectively induced grid-scale subsidence is a strong ~~, but also a slow process . Therefore, it~~ process that has a significant impact on the diagonal below the main diagonal. The values are commonly in the same order of magnitude as in the ~~box~~ boxes above. The descending portions are often even higher ~~as~~ than the ones not affected by convection. For example, more than 90 % of the air that was originally at ~~551.62~~ 552 hPa (level 20) ~~and subsided to 592.81~~ subsided to 593 hPa (level 21).

The large-scale subsidence balances together with the downdraft the updraft in CVTRANS (**?**). The subsidence is formulated in such a way that it is much slower than the updraft. This is realised by reducing the transport distance by allowing the subsidence to transport mass to the model level directly below the original level only (see Equation (2) from **?**). Therefore, this outstanding second diagonal can be seen in the convective exchange matrix in Fig. 3(a).

The upward transport is largest when starting from levels between the ~~lowest level at 937.63 hPa and~~ level closest to the surface at 938 hPa (level 31) and 873 hPa (level 28~~at 873.29 hPa~~) compared to other origin levels. This indicates a huge

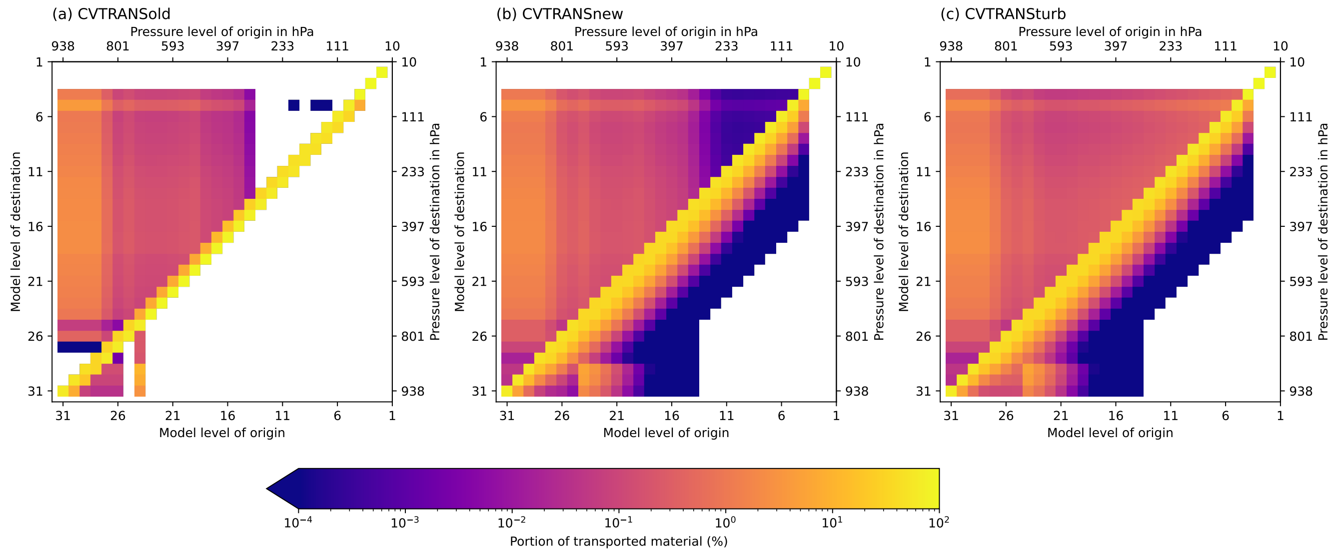

Figure 3. Convective exchange matrix for one snapshot of one specific event. The convective event was located over ~~west~~ Western Australia in ~~south~~ the southern summer (23.316°S, 120.000°E on 1st January 1979 at 5 UTC). The convective exchange matrix is displayed for one time step. (a) shows the convective exchange matrix calculated with CVTRANSold, (b) the convective exchange matrix calculated with CVTRANSnew, and (c) the convective exchange matrix as (b) but with enhanced turbulent mixing (CVTRANSturb).

boundary layer to mid and upper troposphere transport. The upward transport decreases with ~~increasing height of the level of origin~~ decreasing pressure of the starting level for many but not all levels monotonically (moving to the right for different origin levels on the x-axis for the same destination level, depicted on the y-axis). The upward transport to 90 hPa (level 5~~(90.06 hPa~~) makes up ~~to~~ almost 4 %. It is the strongest in the upper troposphere, suggesting that ~~level 5 is~~ the main outflow level of the convective system is located at 90 hPa.

The transport is intermittent in Fig. 3(a). For example, no material is transported from 938 hPa (level 31~~(937.63 hPa) to~~) to 903 hPa (level 29~~(902.65 hPa~~) in spite of the transport from 938 hPa (level 31) to levels above ~~838.82 hPa~~ 839 hPa (level 27). The main organised entrainment is taking place in the region below ~~838.82 hPaand consequently the missing detrainment occurred~~ 839 hPa. The missing detrainment occurs due to the suppression of turbulent ~~detainment~~ detrainment as described above. Also, the upward transport from the upper levels exhibits "missing values" due to a lack ~~in~~ of entrainment in the upper levels, where the organised detrainment is emphasised. This error is corrected in the new version of CVTRANS. Consequently, the transport is continuous in Fig. 3(b).

The transport from level ~~937.63 hPa to 902.65 hPa~~ 938 hPa (level 31) to 903 hPa (level 29) is still small compared with the transport to the levels above ~~838.82 hPa~~ 839 hPa (level 27) in Fig. 3(b). The turbulent detrainment of air in the boundary layer and lower troposphere has implications for the mid and upper troposphere, i.e., less material from the surface level will arrive in the mid and upper troposphere because it is partly detrained below (Fig. 4(a)). Only 3.13 % of the air mass from 939 hPa (level 31) reaches the main outflow level.

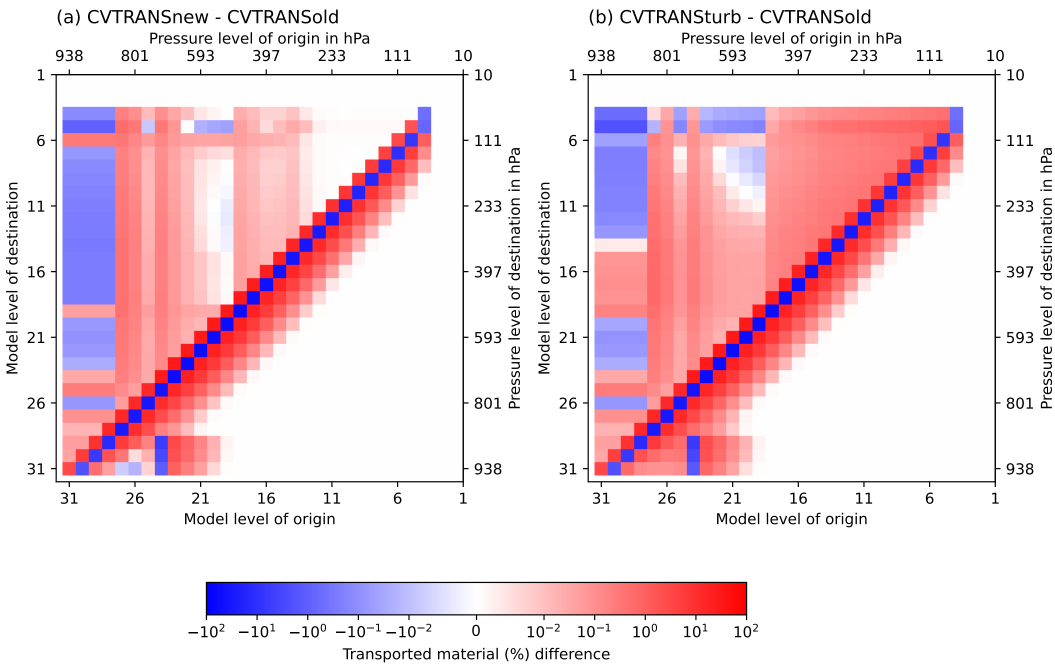

Figure 4. Difference (a) between the convective exchange matrix calculated with CVTRANSnew and the convective exchange matrix computed with CVTRANSold and (b) between the convective exchange matrix based on CVTRANSnew and the one calculated ~~wit~~ with CVTRANSturb.

Partly, material is entrained in the updraft in the upper troposphere due to turbulent mixing~~. The transport portions clearly distinguish the new from the old CVTRANS version~~, but the values are small and ~~therefore the~~ their quantitative impacts are barely noticeable. The downdraft is pronounced when CVTRANSnew is applied. Air mass is shifted to a greater ~~extend~~ extent by the downdraft to the lowermost three levels by CVTRANSnew (Fig. 3(b)) than by the old version of the convective tracer transport scheme (Fig. 3(a)).

The number of side diagonals below the main diagonal has increased ~~comparing~~ compared to Fig. 3(a) with Fig. 3(b). This ~~is~~ can be attributed to the ~~application of the~~ adaptive time stepping ~~according to ?. Thereby, an~~ introduced by **?**. The algorithm chooses as many ~~subtimesteps~~ sub-time steps as necessary in order to avoid mass balancing issues instead of cutting the intense mass fluxes. The adaptive time stepping allows the ~~convection, especially the~~ updrafts to be as strong ~~and as fast as they are given~~ as suggested by the convection parameterisation. Consequently, the ~~large-scale subsidence becomes~~ mass-balancing subsidence is elevated as well and can cover more ~~then one~~ vertical levels, i.e., as many levels as ~~there are substeps required, as the re-distributed mass is calculated for each substep individually, including the large-scale subsidence in each grid cell.~~ intermediate steps are required. This leads to a ~~more smeared~~ broader signal of the ~~large-scale~~ subsidence in Fig. 3(b).

The same snapshot (i.e., identical convective mass fluxes and entrainment and detrainment rates) of a convective system is shown in Fig. 3(c) for high turbulent mixing. The turbulent mixing in this case is enhanced ~~, i.e. , it~~ compared to CVTRANSnew. It is as strong as the ~~maximised turbulent mixing as~~ turbulent mixing suggested by **?**.

The difference in the upper troposphere is substantial when ~~comparing~~ compared to to CVTRANSnew. A distinct larger fraction of material is entrained due to the enhanced ~~turbulence~~ turbulent entrainment into the updraft in the upper troposphere~~into the updraft. Therefore, less~~ . Less material is directly transported from the boundary layer to the upper troposphere. The material is instead detrained already via mixing in the mid troposphere ~~as can be seen in Fig.4(b~~(Fig. 4). It can be assumed, given that bulk formulations tend to transport material less ~~efficient~~ efficiently to the upper troposphere, as the more complex plume ~~ensemble based~~ ensemble-based approaches (**?**) that the transport to the upper troposphere by CVTRANSturb is not efficient enough.

The goal of the modifications is to overcome the issues with the missing turbulent mixing and not to alter the results of the simulations strongly from the original version, as it is the case for CVTRANSturb because **?** showed already that CVTRANSold reproduces observed vertical tracer profiles. Therefore, in Sec. 3.2 CVTRANSnew is applied to investigate historical changes in the convective transport characteristics, because the deviations between CVTRANSnew and CVTRANSold are smaller than the ones between CVTRANSturb and CVTRANSold.

3.2 Convective transport trends

We performed nudged EMAC simulations including CVTRANS 3.0 ~~starting in~~ (configuration $\text{CVTRANS}_{\text{new}}$) from January 1979 to December 2020. ~~Of this time period~~For reducing spin-up and initialisation effects, the first year is ~~excluded from the analysis to reduce spin-up effects. The~~ discarded, such that the convective properties and the convective transport are ~~considered in the analysis for~~ analysed for the period from 1980 to 2020. This time period is sufficient to give a first impression ~~about~~ of the climate response of the modelled convective transport~~since climate signals become recognisable on time scales of 30 years. The investigations are~~ . The analysis is only performed between 60°S and 60°N because this is the area ~~,~~ where convection is of high relevance.

Remark: ~~In the analysis, the~~ The transport is discussed referring mainly to model levels and not pressure levels ~~. This is due to the fact, that~~ because the pressure varies largely between the boxes mainly due to orography and secondary due to weather systems. A re-gridding is not possible in a convincing manner, as interpolation artefacts would, i.e., violate the mass balance~~and the mass redistribution~~. We try to refer to specific areas in the atmosphere as ~~for example the UT or the mid troposphere~~boundary layer, free troposphere, upper troposphere, and lower stratosphere for a better understanding, but ~~please keep in mind that these areas vary as well with orography and furthermore with latitude.~~ these depend as well on orography and the latitude. The reader is referred to Table S2 to get an impression of the tropopause height and the boundary layer height in the model. The equivalent pressure is presented alongside the model levels to allow a rough estimation of the pressure. This equivalent vertical pressure is based on a vertical profile where the pressure in the box closest to the surface is 1013 hPa.

3.2.1 Global changes

The convective transport matrix is shown in Fig. 5 for the temporal mean of the ~~ten year~~ ten-year period 2011 to 2020 and the ~~area weighted~~ area-weighted mean between 60°N and 60°S. The mean transport matrix is shaped by a large number of initial unit matrices because atmospheric moist convection is a rather localised effect. As a consequence, the mean convective transport is of cause not as intense on a global scale as for ~~a~~ an individual local event (compare Fig. 3(a)). Nevertheless, the convective transport has a non-negligible effect on large spatial and temporal scales.

The ~~convective transport based on the Tiedtke-Nordeng convection parameterisation indicates typical features. The~~ strongest upward transport starts in the lower free troposphere and in the boundary layer (level 31 to 26) and ~~reaches not~~ does not reach very far into the free troposphere (level 29 to 25), representing shallow convection and turbulent detrainment from updrafts. Deep upward transport starts mostly in the same area (levels 31 to 28), but shows lower fractions as the transport into the lower free troposphere. ~~Higher starting levels~~ Starting levels in the free troposphere are associated with lower portions of upward transported material.

The ~~large-scale subsidence is obvious over two to three levels as~~ mass-balancing subsidence is the dominant downward transport mechanism over two to three levels below the main diagonal. ~~Also the effects by downdrafts is striking.~~ For the lower to ~~mid tropospheric~~ mid-tropospheric origin levels, the downdrafts ~~lead to a clearly distinguishable increase in the transported mass portion to the lowest three model levels on a global scale~~transport air mass especially to the three levels closest to the surface.

Figure 6 shows the temporal and spatial mean convective transport compared between 2011 and 2020 to the reference period from 1980 to 1989. The transport to ~~the upper~~ lower pressure levels increased significantly. The upward transport has strengthened to ~~the level 4 to 7,~~ levels at about the height of the tropical tropopause ~~,~~ (level 4 to 7) from all starting levels below the destination levels. ~~In the mid latitudes, these height levels are located in the stratosphere and are only occasionally influenced by deep convection. The large-scale~~ The subsidence adapted accordingly. More material descents from levels which are associated with the upper troposphere in the tropics and with the upper troposphere and lower stratosphere in the ~~mid latitudes~~ mid-latitudes (between level 12 and 4).

These features of the difference convective exchange matrix (Fig. 6) can be explained considering the frequency distributions of the updraft mass fluxes compared for the reference time period and 2011 to 2020 (Fig. 7). In Fig. 7, the mass fluxes from deep convective events were categorised according to their strength. The lowest class (below $1 \times$ ~~-~~10^{-7} kg m^{-2} s^{-1}) contains all ~~no events~~no-events, so the cases where no deep convection occurred or the mass fluxes were ~~to~~ too small. The class with the strongest updraft mass fluxes contains all mass fluxes which are stronger than 0.2 kg m^{-2} s^{-1}. This classification was performed for all height levels. The difference of these mass flux distributions is shown in Fig. 7 for a selected set of model levels and for the values from 2011 to 2020 minus the ones ~~of~~ from 1980 to 1989. For a better visualisation, the symmetric logarithmic difference is shown instead of the absolute numbers.

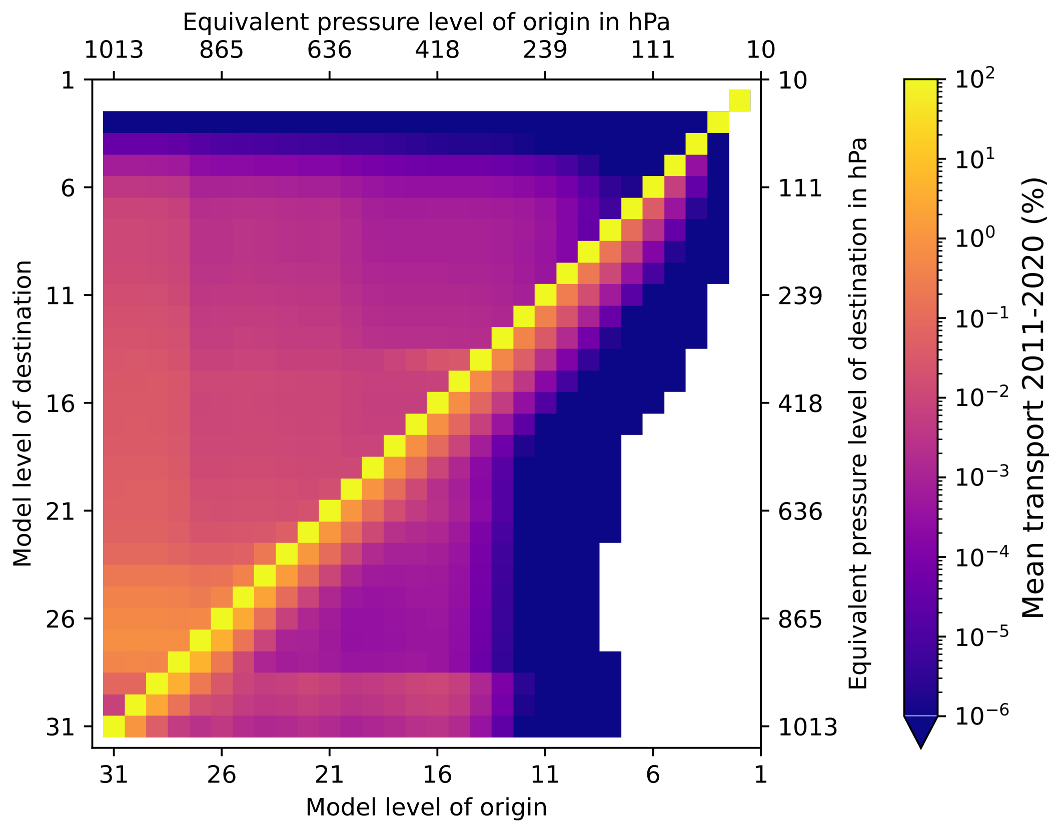

Figure 5. Area weighted between 60°N and 60°S and temporal mean convective transport matrix, i.e., the fraction of air mass which was transported from ~~a~~ an origin to a source level, for 2011 to 2020. Note that the equivalent pressure (upper and right axis) is determined from a standard atmosphere over the ocean with zero orography.

The updraft mass flux in the upper levels (height range of the tropopause) shifts to stronger mass fluxes in the later time period. Moreover, more events ~~reaching up to higher~~ reached these levels from 2011 to 2020 in comparison to the reference period. This trend is ~~consisted~~ consistent with the increased transport to the upper level as observed in Fig. 6.

The enhanced transport to ~~higher levels~~ levels roughly associated with the tropical tropopause could be explained by an increase in the strength of the convection or even an enhancement of convection overshooting the tropopause. A non-significant tendency towards more overshooting convection is predicted by the Tiedtke-Nordeng scheme over the ~~41 year~~ 41-year time period. ~~Thereby, overshooting is defined as events where~~ We define one (tropopause) overshooting event as an event when the updraft mass flux ~~reached beyond the~~ associated with one convective event reaches beyond the independently calculated tropopause in one column and at the same time step. It cannot be ruled out that the detected overshooting is only an artefact of the coarse model resolution because both ~~,~~ the tropopause height and the mass flux are mean values. It can be assumed that

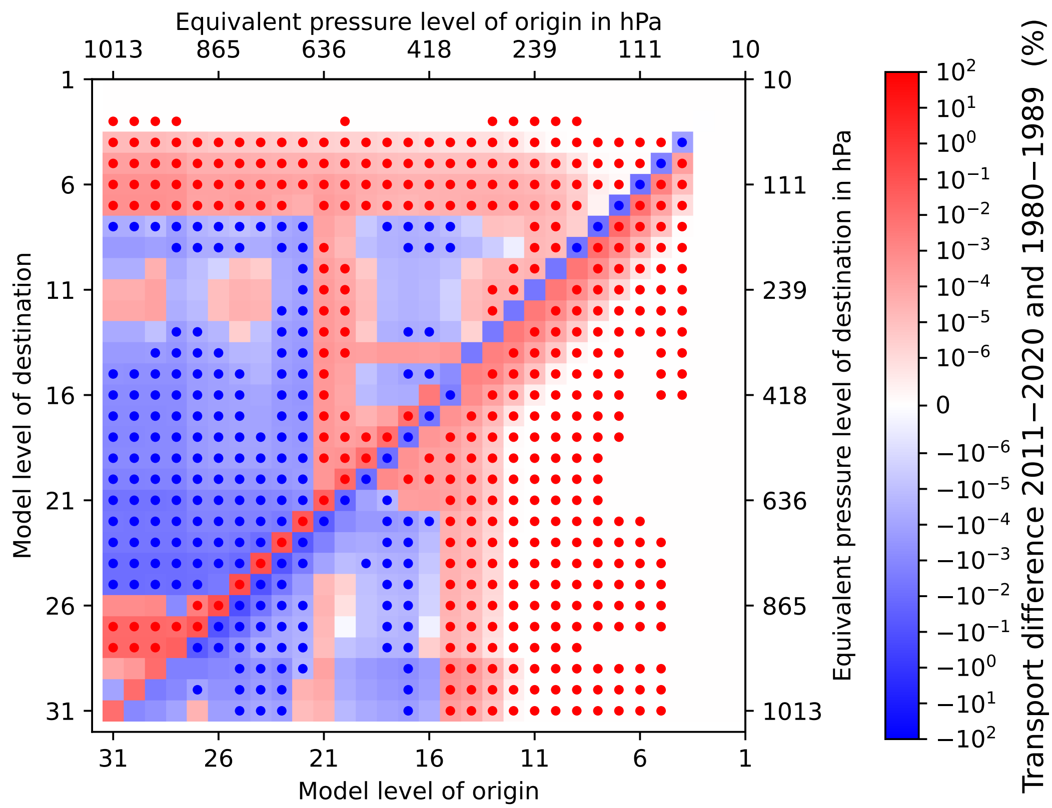

Figure 6. Changes in the convective mean transport between 60°S and 60°N. The temporal (~~ten year~~ten-year) and global (~~area weighted~~area-weighted) convective exchange matrix is compared from 2011 to 2020 and from 1980 to 1989. Red colours denote that the values were higher in the period 2011 to 2020 and blue boxes show that the entry in the convective exchange matrix was higher from 1980 to 1989. A dot in a box indicates statistical significance. A ~~two sided~~ two-sided student t-test was used with a significance threshold of 1 % for every side of the t-distribution.

both quantities vary significantly within a box. However, the latter does not affect the convective transport in the model because the transport only sees the grid box mean values.

~~? found an increasing trend in tropical overshooting convection based on simulations from 1979 to 2008 and based on satellite obeservations from 1998 to 2013.~~ ? discovered that tropical convection reaching beyond the tropical cold point tropopause occurred slightly more often in the future scenario (2075-2104, Intergovernmental Panel on Climate Change A1B emission scenario) than in their historical simulations (1979-2008). Concerning this study, ~~convective tropopause overshooting~~ the trend in tropopause overshooting convection is not significant. Therefore, it can be ruled out as primary source for the major increased convective transport to the ~~levels~~ tropical tropopause / lower stratosphere levels (level 7 to ~~4. The impacts of the overshooting on this trend are negligible due to the small and non-significant changes in overshooting in our simulation.~~ 4).

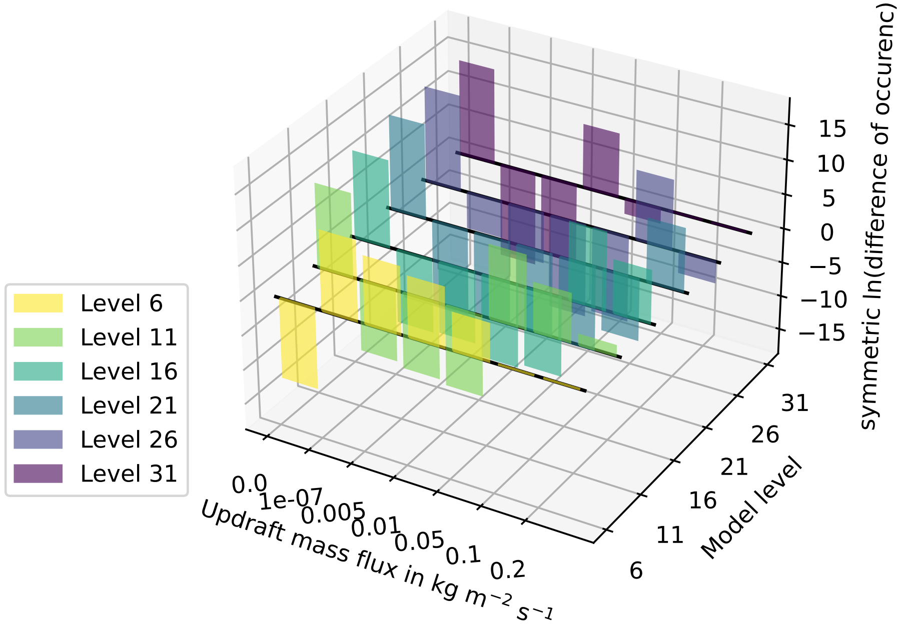

Figure 7. The distribution of the updraft mass fluxes is given as the symmetric logarithmic difference between the absolute frequency distributions ~~of~~ from 2011 to 2020 ~~and~~ minus the one from 1980 to 1989. The ~~colors~~ colours denote different altitude levels. Updraft mass fluxes are divided into seven categories. Updraft mass fluxes below $1 \times$ ~~−~~10^{-7} kg m^{-2} s^{-1} are not considered in the transport routine CVTRANS. Therefore, these mass fluxes are in the smallest category and are considered as no occurrence of convection.

The model predicts an increase in the global mean tropopause height (not shown). A higher troposphere could clear the path for convection with a larger vertical ~~extend~~extent, but an increased penetration of convection could also cause a rise of the tropopause height (for the second possibility, see **?**). Deep convection tends to occur less ~~frequent~~ frequently (Fig. 8) and for this reason the increased height of the deep convection has ~~only rather locally an~~ a rather local impact on the tropopause height. Therefore, we assume that the dominating process ~~here~~ is the change in tropopause height~~leading~~ , which leads to deeper convection and not vice versa.

The upward transport has decreased from ~~the starting levels~~ starting levels in the lower troposphere (levels between 31 to roughly 21) to the destination levels in the mid troposphere and some upper ~~tropospheric levels in the later time period~~ troposphere in the most recent time period in comparison to the 1980s (see Fig. 6). ~~Fig.~~Figure 7 is considered again to examine possible reasons for this decrease in upward transport. ~~Less deep~~ Deep updraft convective mass fluxes ~~are counted in the period from 2011 to 2020 in comparison to the 1980ies~~ occurred less frequently in many height levels with relevant values (larger $1 \times$

~~-~~$10^{-7}\,\mathrm{kg\,m^{-2}\,s^{-1}}$) ~~. However, a~~ from 2011 to 2020 in comparison to the 1980s. A bimodal trend emerges from Fig. 7 in terms of the changes in the distribution of the deep updraft mass fluxes. The mass fluxes tend to be either at the stronger edge or ~~very close to~~ zero in the later time period. ~~In level 6, higher~~ Higher mass fluxes are generally favoured in the ~~later period~~uppermost levels in the later period, shown in Fig. 7 (level 6). Therefore, the negative trend in some upper tropospheric levels in Fig. 6 can ~~partly~~ be attributed to an increase in the outflow height ~~. In addition,~~ and a decreasing trend in the occurrence of deep convective events over the 41 year period ~~is determined~~ (Fig. 8).

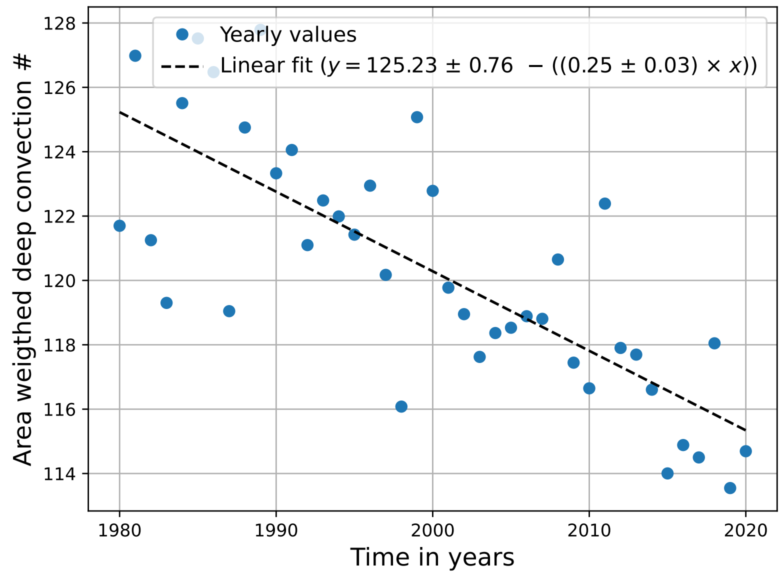

Figure 8. Normalised time development of the ~~area weighted~~ area-weighted deep convection events per year. The ~~crosses~~ blue circles denote the yearly number of convective events and the dashed line is the linear fit of the ~~area weighted~~ area-weighted deep convection events. x denotes the number of relative years~~,~~; thus, x is equal to zero for 1980. The standard error of the slope and the intercept are given for the linear fit. y is the number of ~~area weighted~~ area-weighted deep convective events per year.

The upward transport increased for ~~the starting levels~~ two starting levels in the mid troposphere (levels 20 and 21) in average from 2011 to 2020 compared to the reference period depicted in Fig. 6. This leads to the hypothesis that ~~mid level~~ midlevel convection occurred more frequently~~in the later time period but the mid level~~; however, midlevel convection according to the definition in the Tiedtke-Nordeng scheme did not increase in number (not shown). ~~Therefore, an increase in the frequency of the midlevel convection can not be the reason, but the penetration height of the convection might. Not only the deep convection reaches higher in the later time period, but also the shallow convection. The~~ On the other hand, shallow updraft mass fluxes tended to higher values in ~~level~~ the two mentioned mid-tropospheric levels (levels 20 and ~~level~~ 21~~(free troposphere~~). The same is the case for the midlevel convection. However, the midlevel convection headed towards a more frequent occurrence of the higher ~~massfluxes~~ mass fluxes for a wide range of altitude levels. These could play a role ~~for~~ in this prominent increase of upward transport from ~~two of the free tropospheric~~ these two mid-tropospheric levels (level 21 and 20). Nevertheless, the ~~cause~~ reason for this cannot be conclusively clarified at this point.

The downdrafts shift to ~~higher starting levels~~ starting levels located higher above the surface in the later time period compared to the reference period (Fig. 6). On the one hand, the impact of downdrafts starting at the mid to upper troposphere (levels 15 to 13~~has increased in the later time period~~) has increased. On the other hand, the downward motion is reduced for origin levels ~~between 26 and 16 (representing the free troposphere in the tropics and the upper troposphere in the higher latitudes) in case of the mean value~~ in the free to mid troposphere (between 26 and 16) in average from 2011 to 2020. This finding goes well along with the height increase of the deep convective systems.

A strengthening of the updraft detrainment is observed in Fig. 6 in the lower troposphere (up to level 26). This could be due to an increase in shallow convection because of the water vapor and lapse rate feedback on convection (e.g., **?**, and references therein). However, the global occurrence of shallow convection did not significantly increase during the ~~41 year~~ 41-year period (not shown). This means ~~,~~ that either the shallow convection intensifies or the detrainment of mid level and/or deep convection must increase.

In total, more material stays ~~in~~ at its original level for levels in the boundary layer to ~~mid troposphere~~mid-troposphere. This trend is ~~for many mid tropospheric~~ significant for many mid-tropospheric levels (between ~~level 17 and~~ levels 27 ~~) significant~~and 17). This also points towards an overall reduced deep convective transport.

3.2.2 ~~Zonal~~ Tropical and extra-tropical trends

~~In Fig. ??~~ Figure 3.2.2(a) shows the difference convective exchange matrix ~~is shown~~ for 30°N to 30°S. Overall, the changes in tropical convective transport match well with the ones for the global case (Fig. 6). The convective transport increased to levels ~~above~~ up to the tropical tropopause (level 7 and above) from 2011 to 2020 in comparison to the ~~1980ies~~1980s. The downdrafts shift as well to ~~higher starting levels~~ starting levels located further up with regard to the surface, and more ~~large-scale subsidence is observed~~ mass balancing subsidence is found for the upper tropospheric to lower ~~startospheric levels. As in the global case~~stratospheric levels. In total, more material stays ~~in~~ at the starting level and is not affected by the convection for a ~~huge~~ substantial number of levels. ~~The convective transport increases compared to the reference period in the lowermost three levels. This is the only distinct difference~~ There is only one dissimilarity between the tropical and the global ~~trends. Overall, the trends in the tropics match well with the ones discussed for the global case~~case: The significance of convective transport differences compared to the reference period in the boundary layer (level 31 to 29) increased.

The picture arising for the Northern and Southern Hemisphere extra-tropics seems to alter from the tropical one (Fig. ~~??) with the global picture~~3.2.2(b) and (c) compared with Fig. 3.2.2(a)). The upward transport is pronounced for a wide range of ~~upper troposphere to lower stratospheric levels(levels 15 to 6) in the later time period in the mid-latitudes of the Northern hemisphere. This is related to the tropopause height~~ levels. However, the tropopause is located mostly at higher pressures in the extra-tropics ~~. The tropopause height varies extensively between 30° and 60° and ranges from similar heights as~~ than in the tropics ~~down below level 16.~~

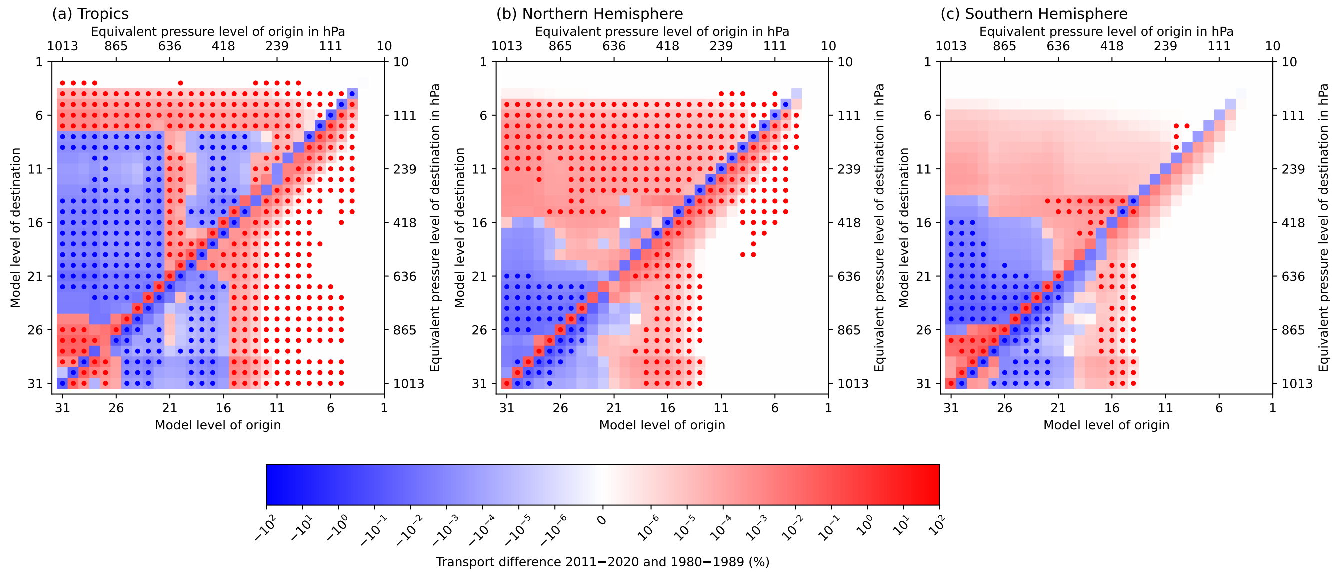

~~The differences in the time development are quite different when comparing the Northern hemisphere between~~ , (b) for 60°N to 30°~~N and~~ N and (c) for 60°~~N~~ S to 30°S.

~~The differences in the time development are quite different when comparing the Northern hemisphere between~~ , (b) for 60°N to 30°~~N and~~ N and (c) for 60°~~N~~ S to 30°S.

Figure 9. Changes in the convective mean transport in ~~the tropics~~different regions. Same as Fig. 6 but ~~between~~ (a) for 30°S and 30°N~~.~~ ~~The differences in the time development are quite different when comparing the Northern hemisphere between~~ , (b) for 60°N to 30°~~N and~~ N and (c) for 60°~~N~~ S to 30°S.

~~A similar picture is emerging for the Northern hemisphere and the global case keeping the difference in tropospheric expansion in mind. Less material is transported upward to a variety of height levels in the lower to upper troposphere (between level 30 and 16). The pattern is quite similar to the global case, but an increased transport to the lower troposphere (levels 26 to 28) becomes apparent when comparing the different decades globally which is not obvious on the Northern hemisphere. The changes~~ (Fig. 2 and Table S2). Considering the differences in tropopause height, the main patterns in convective transport ~~on the Northern hemisphere~~ changes are similar in ~~three other aspects to the trends on the global scale~~all considered regions compared to the latest ten years of the simulation with the 1980s: (1) The ~~downdrafts shift to higher origin levels~~convective transport to the tropopause region and above is increased. (2) ~~Less air mass transport is ongoing in the lower levels from 2011 to 2020 in comparison to 1980 to 1989. This is indicated by the positive changes in Fig. **??** on the main diagonal for a wide range of the lower and mid troposphere (levels 31 to 22). The transport increased above level 22 (mainly in the upper troposphere)~~The mass balancing subsidence strengthened from origin levels at about the tropopause height / lower stratosphere. (3) The ~~large scale subsidence is enhanced in the upper levels.~~

~~Northern hemispheric changes in the convective mean transport in the tropics. Same as Fig. 6 but for 60°N to 30°N.Southern hemispheric changes in the convective mean transport in the tropics. Same as Fig. 6 but for 60°S to 30°S.~~

~~The differences of the convective exchange matrix in the Southern hemisphere for the two time periods are shown in Fig. **??**. They are small when compared to the changes in the tropics and in the Northern hemispheric extra-tropics. Between 2011 and 2020 the convection tends to reach higher than in the reference period, but these changes are not statistically significant. The contrast between the changes on the Southern hemisphere and the Northern hemisphere can be attributed to the unequal distribution of land mass on both hemispheres, and therefore the lacking of intense continental mid-latitude convection.~~

~~Many transport processes changed although significantly in the levelsbelow level 17 (mainly tropospheric levels). A shift of the downdrafts occurred qualitatively analogue to the global case (Fig. 6) . The upward transport to the lower free troposphere (below level 26) increased and the transport of air originating at the same starting levels and reaching the~~ downdrafts originate at higher levels~~26 to 16 (mid~~. (4) Less material from the boundary laxer / lower troposphere reaches the free to upper troposphere ~~) is often significantly reduced. This is in good agreement with the findings on the global scale. It also supports that deep convection is suppressed more frequently in the later time period than in the reference period in the simulations~~(up to level ~16).

~~We conclude that the Northern and Southern hemispheric changes are qualitatively compatible to the global and tropical changes taking the differences in the respective tropopause heights into account. However, the changes on the Southern hemisphere~~ Thereby, the convective transport changes are not as ~~significant as the ones~~ often significant and as much pronounced on the Southern as on the Northern ~~hemisphere and in the tropics~~Hemisphere.

3.2.3 Regional differences

~~The vertical transport of air masses is strongly influenced by the location of the convective events. Therefore, the~~ The mean convective transport from the boundary layer (BL) to the upper troposphere (UT) is calculated for each grid column to assess the regional variability of convective transport. The upper troposphere is heuristically defined as the region ~~including the level of the tropopause~~ vertically ranging from the tropopause level (in hPa) down to the level where the pressure is equal to the tropopause pressure plus 150 hPa. The tropopause height and the height of the planetary boundary layer are taken directly from the EMAC output.

The mean upward transport is not directly comparable to a tracer concentration in the UT or tracer release studies as performed, e.g., by **??** or **?**. Different processes interplay and impact the transport of a tracer. The convective exchange matrix opens the possibility to study the upward transport driven by convection undisturbed by other processes and pre-existing tracer distributions. In this section, the focus is on the regional differences and "trends" of the ~~consecutively induced~~ upward transport from the BL to the UT.

The ~~ten year~~ ten-year mean of the BL to UT transport is shown in Fig. 10. The convective transport shows a similar structure as the convective precipitation (compare, e.g., **?** and **?**, their Fig. 8) and the cloud top brightness temperature (compare **?**). The values are enhanced in the inner tropical convergence zone, Amazonia, ~~central Africa~~Central Africa, and the North Atlantic storm track. No air masses were transported from the BL to the UT ~~westerly~~ West of Africa and South America, where

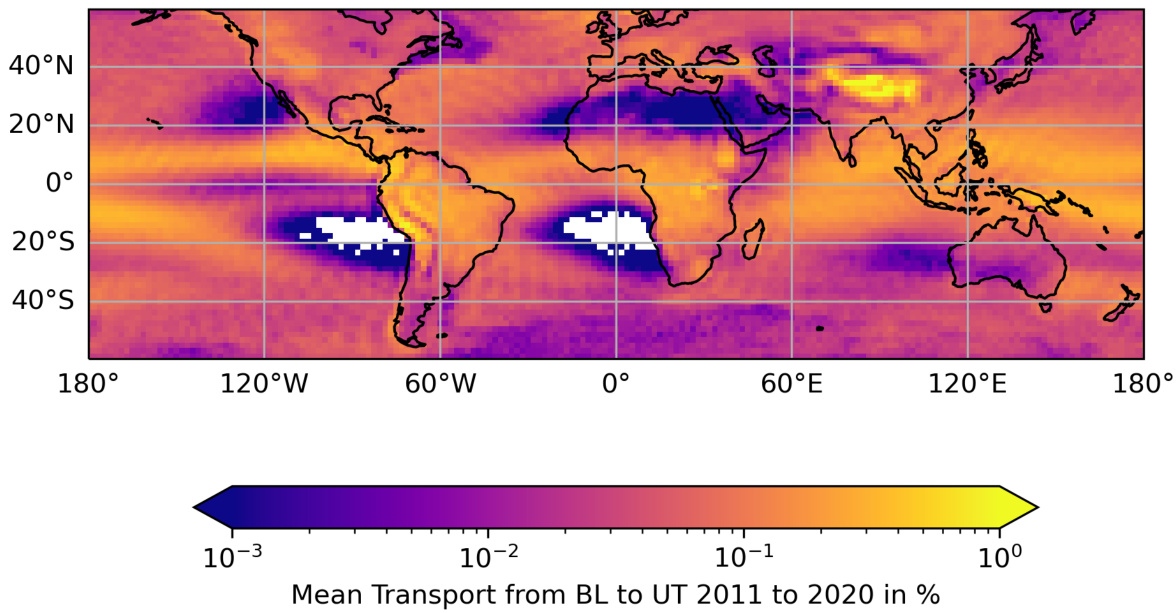

Figure 10. ~~Ten year~~ Ten-year (2011 to 2020) mean convective mean transport from the planetary boundary layer height to upper troposphere within 12 min. The upper troposphere is defined as the vertical region between the tropopause and the ~~pressure~~ height of tropopause in hPa plus 150 hPa.

subsidence is dominating the large-scale circulation patterns. Small but ~~none zero~~ non-zero values indicate very low (deep) convective activity ~~westerly of Australia. This is also the case~~ West of Australia, over North Africa, and off the coast of California.

Particularly high portions of air mass were transported from the BL to the UT above the Himalaya and the North to ~~central~~ the Central Andes mountains. This is for two reasons not surprising: (1) The model levels are compressed above high mountain areas. Thus, the distance between the BL and the UT decreases accordingly. (2) ~~The~~ It can be assumed that the Tiedtke-Nordeng scheme does not perform sufficiently well in these areas in general, because the precipitation rates calculated with the Tiedtke-Nordeng convection parameterisation within EMAC are to high compared to observations in these areas, as shown by **?** in their Fig. 2. ~~It can therefore be assumed that the convective transport is as well overestimated based on the Tiedtke-Nordeng scheme in those regions~~As the freshly formed precipitation is proportional to the updraft mass flux, a too strong updraft mass flux results in both an overestimation of the convective precipitation and of the convective upward mass transport.

~~The redistribution of air masses due to convection has changed significantly over the past decades as shown in Subsec. 3.2.1. However, the~~

The change in the mean BL to UT transport is characterised by regional differences (see Fig. 11). In dependence of the region, the trend is either negative or positive.

~~As Fig. 10 but for the difference of the mean values of 2011 to 2020 and 1980 to 1989.~~

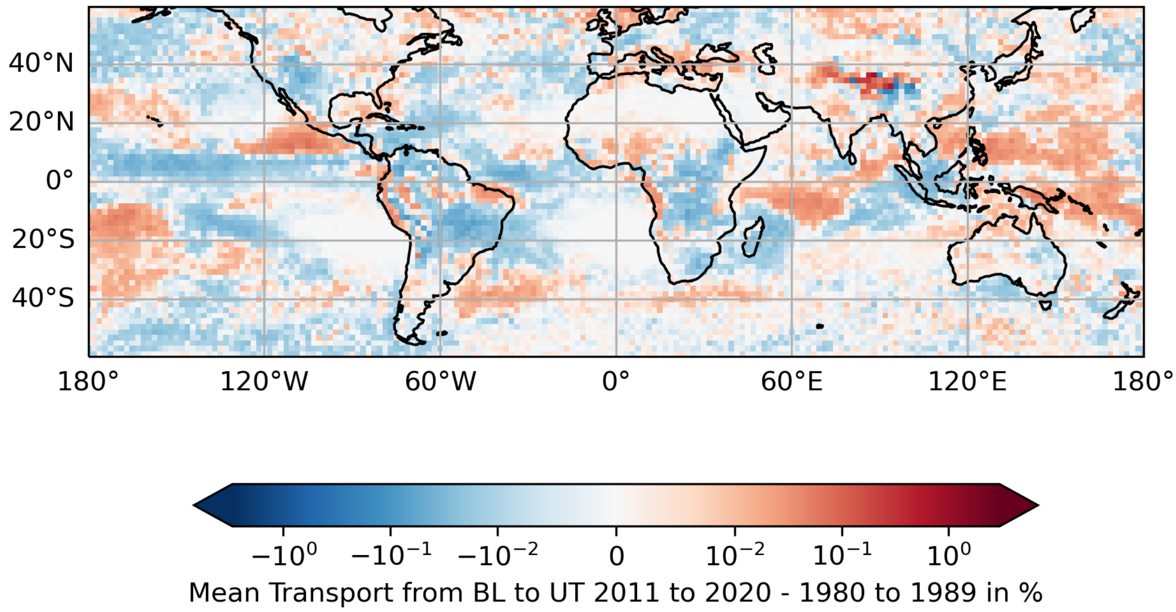

Figure 11. As Fig. 10 but for the difference of the mean values of 2011 to 2020 and 1980 to 1989.

Overall, the transport from BL to UT was only slightly smaller between 2011 to 2020 than in the reference period. The global (60°S to 60°N) area weighted average decreased from 0.07909 % per time step (1980 to 1989) to 0.07829 % per time step (2011 to 2020). This seems ~~counter intuitive~~ counter-intuitive at first glance because of the significant increase of transported air masses to the upper levels of the convective exchange matrix (compare Fig. 6). First and foremost, the increase of the convective outflow height leads to the increased transport to the ~~levels 5~~ uppermost levels influenced by the convection (levels 4 to 7) (in Fig. 6), likely due to an increase in the tropopause height. That does not necessarily imply an increased transport into the whole UT. ~~The transport matrix shows instead that in many levels a larger portion of the air mass stays in the original level in the average between 2011 to 2020 as in the reference period.~~

The mean transport from the BL to the tropopause region remains nearly unchanged. Thereby, the region of the tropopause is defined as the ~~the~~ level of the tropopause down to the level with a pressure equal to the pressure at the tropopause plus 50 hPa (in contrast to the UT, which was defined by the tropopause pressure + 150hPa). The mean transported portion was 0.02114 % per time step in the reference period and increased marginally to 0.02118 % per time step ~~in~~ from 2011 to 2020. This indicates that less convection reaches the upper troposphere in general, but that the convective transport to the tropopause region stays similar due to compensating processes: The deeper penetration balances or even exceeds the effect due to the lower occurrence rate of deep convection. We note that these trends are rather small and need to be validated in the future.

The transport to the UT decreases close to the equator over the eastern Pacific. An increase becomes apparent North and partly also South of the equatorial region over the Eastern Atlantic. A possible weakening and widening of the Hadley cell (**??**) could explain this trend. In this framework, we cannot confirm or reject this hypothesis.

The problems of the underlying convection parameterisation ~~is~~ are an important factor for the convective transport as well. The regions with the largest changes are widely the areas of the least accurate ~~predictions~~ simulations of precipitation by the Tiedtke-Nordeng convection scheme. This convection parameterisation overestimates the precipitation at the ~~pacific cost~~ Pacific coast of Central America, Central Africa~~and the western Pacific and western~~ , and the Western Pacific and Western Indian Ocean and underestimates the precipitation over the ~~western Maritime continentas can bee~~ Western Maritime continent, as can be seen in Fig. 2 by **?**. These areas show pronounced changes in the transport of BL air to the UT. These changes~~go therefore~~, therefore, go along with high uncertainties, which we cannot further quantify due to a lack of global observations of convective transport or mass fluxes.

3.2.4 Natural variability in convective transport

~~To conclude~~ To analyse whether the regional changes originate from climate change or are due to natural variability~~the intra-decadal variability is studied using extreme states. One El Niño event is compared to one La Niña event to investigate~~ , one La Niña event (Fig. S3) is compared with one El Niño (Fig. S4) event to estimate the maximal variability ~~which~~ that can occur within one decade. For the El Niño event, July 1st, 1982 to June 30st, 1983 was chosen because **?** identified ~~this event~~ it as an extreme ~~El Niño~~ event. According to **?**, a strong La Niña event took place in 1988 and ~~1989. This event is used for the analysis.~~ 1989, which is chosen as conditions very different from the El Niño event. For consistency reasons, we took the second half of 1988 and the first half of 1989 ~~into account~~ for the La Niña case ~~.~~

~~The La Niña event (Fig. S4) has similar patterns as the ten year mean (Fig. 11). That was to be expected because La Niña is characterised by a strongly pronounced Walker circulation. In contrast, the direction of the circulation changes in the El Niño case (Fig. S5) leading to large differences in the convective transport patterns. These are especially large over the central Pacific. In the La Niña case, partly no deep convective transport was active at the equator in the considered time period. In contrast, BL to UT transport stands out during the El Niño event in exactly this region.~~ into account.

The largest differences between the El Niño and La Niña event occurred in the area of the equator over the Pacific. The mean transport to the UT from BL differs up to 0.38~~% per timestep in the area of the equator over the Pacific~~ % per time step (Fig. 12). **?** found an increased number of organised convective events in the same area comparing El Niño events with La Niña events between mid of 1983 and mid of 2008. This matches with the presented results from this study, that there is more transport into the UT from BL during the considered El Niño event. A huge decrease can be observed North and Southwards from the equator in the Pacific and over the maritime continent when comparing the El Niño event from 1982/83 with the La Niña event 1988/89 (~~see~~ Fig. 12). ~~The deep convective transport is also less active in the El Niño case over the maritime continent. This again is in good agreement with the findings of **?** (their Figs. 3 and 4) concerning the occurrence of organised convection.~~

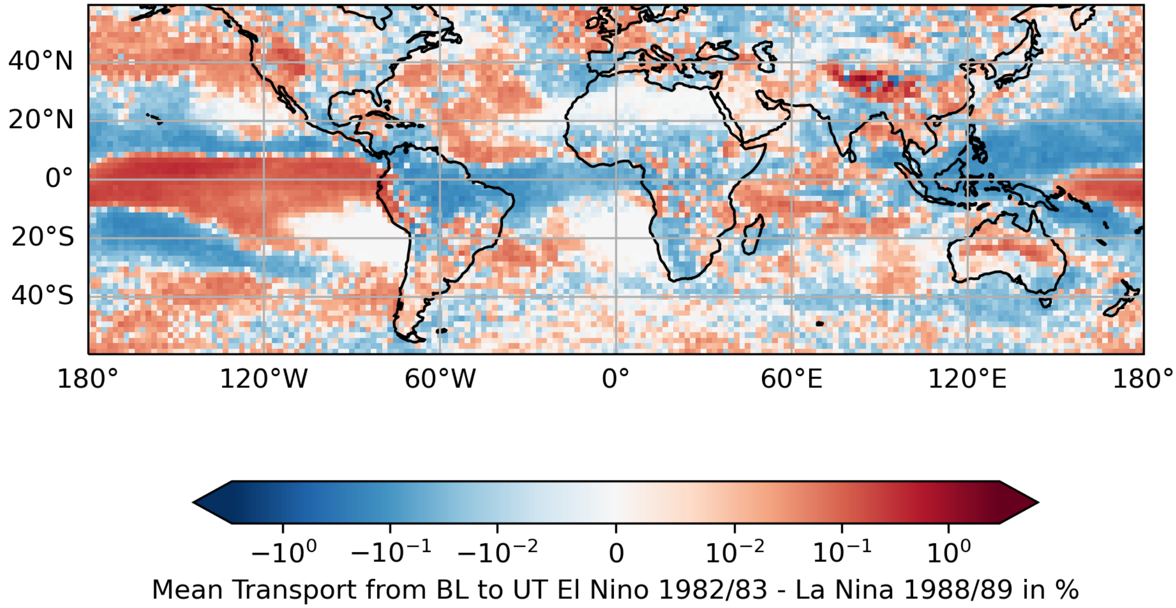

~~As Fig. 10 but for the difference between the el nino event 1982/83 and the la nina event 1988/89.~~

Figure 12. As Fig. 10 but for the difference between the El Niño event 1982/83 and the La Niña event 1988/89.

~~There are also huge differences over the equatorial Atlantic, the North-Western Atlantic and the Northern and Southern Pacific (Fig. 12). The differences in convective transport are striking when comparing~~ Overall, the differences between the El Niño ~~event with~~ and the La Niña event ~~. They~~ are much more pronounced than ~~the differences which appear in the comparison of the ten year mean values (~~changes in Fig. 11~~). Overall, there is no clear trend associated with the climate change in the convective BL to UT transport on regional scales, which exceeds the maximal variability within a decade.~~ .

4 Discussion

In Sec. 3.2.1, a rather small sample size is used to identify climate changes ~~. To underline the significance of the global trend, we investigated also the time periods~~ in convective activity. We investigated the periods from 1990 to 1999 and from 2000 to 2009 and compared them to the reference period (Fig. ~~S2~~ S1 and Fig. ~~S3~~S2) to further substantiate the discussed changes ~~in the convectively induced~~ of the redistribution of air masses. The ~~time period 1990 to 1999 shows similar~~ changes in the convective transport ~~in comparison to the reference period from 1980 to 1989 as the latest considered time period. The trend is quantitatively much smaller but in terms of the qualitative changes comparably. The differences become more significant for the time~~ patterns are not as significant when comparing 1990 and 1999 to the 1980s, but qualitatively similar to Fig. 6. The similarity to Fig. 6 is even more evident for the period from 2000 to 2009 compared with the reference period. ~~They are still not~~

~~as pronounced as in Fig 6. Therefore, we conclude that the trend of the change is strengthening with time and~~ Therefore, the trend is consistent over the decades ~~with an increasing amplitude~~ and strengthens when the climate change signal intensifies.

~~The~~ However, the temporal changes in the mean BL to UT transport are small on a regional scale in comparison to the maximal inner decadal variability ~~on a regional scale in the past four decades.~~ induced by El Niño and La Niña events~~can lead to a huge natural variability of the regional convective transport efficiency within a decade. As a result, the trends in the background state appear partly masked by the high natural variability~~.

~~This study focuses on the representation of convective transport based on~~

Further uncertainties arise from the use of a convection parameterisation~~in an global circulation model. The Tiedtke-Nordeng convection parameterisation is based on basic physical principles, but is as all parameterisations a simplification of processes. Uncertainties arise from the use and~~. Moreover, the results might depend on the choice of ~~each individual convection parameterisation. The convective transport differs for specific events when different convection parameterisations are used (**?**). We did not investigate how strongly the results of this study depend on the applied convection parameterisation~~the convection parameterisation, because the convective transport of individual events depends on the convection scheme (**?**). Therefore, this analysis can ~~give an hint, how convection in general might behave but cannot provide any~~ provide a first hint, but no reliable information about the convective transport outside ~~of~~ the model framework of EMAC ~~under the use of~~ with the Tiedtke-Nordeng convection scheme.

~~Furthermore, uncertainty arises due to the nudging~~ The nudging can introduce uncertainties as well because the ERA5 data already include convective processes. This might lead to less unstable conditions and ~~therefore,~~ might influence the triggering of convection in the model. This process was investigated in further detail by **?**. **?** also discussed that ~~the nudging also~~ nudging influences the tropopause height. ~~Nudging~~ We can not avoid these issues, because nudging is necessary to perform a transient simulation as close as possible to the real world or at least to the reanalysis. ~~Therefore, we can not avoid this issue.~~ To test the robustness of our results, we performed another simulation~~where we only nudged~~: Only the surface pressure ~~,~~ was nudged and the sea surface temperature~~and~~, the sea ice coverage ~~. Furthermore, only~~ were prescribed, and climatologies were applied for the aerosol and ~~green house~~ greenhouse gas forcing. The tropopause height is strongly affected in a quantitative sense. Nevertheless, neither the trend of the tropopause height nor the trends concerning the mean convective transport change qualitatively. ~~We can therefore assume that influence of the nudging on the trends is minor.~~

Our results are to some ~~extend consisted~~ extent consistent with other studies. An increase of the tropopause height / ~~an~~ a decrease of the tropopause pressure has been already determined in several studies, for example, via radiosonde observations for the tropics by **?** and for the Northern hemisphere by **?**, via reanalysis data by **?** and ~~?~~ **?** (only for the Northern hemisphere) and by performing a ~~mulitmodel intercomparison~~ multi-model inter-comparison (**?**). Based on satellite data, **?** and **?** observed ~~an~~ a rising of the top height of high clouds in the tropics ~~what gives us confidence with regard to the deeper convective clouds determinedhere. Also? detected applying idealised~~ which goes well with the deeper convection we determined. Also, **?** concluded from simulations that convection ~~reaches further~~ penetrates deeper with higher sea surface temperatures.

~~The trends in convection are still under discussion.~~ **?** discovered a wide-ranging decreasing trend in thunderstorm environments based on ERA5 data. Their calculated severe thunderstorm hours show a decrease for the ~~mid latitudes, but~~ mid-latitudes, but a partly an increase in the tropics. On the other hand, **?** found an increasing trend for severe storms across various regions using proxies based on CIMP6 projections.

? found that the updraft speed can strengthen up to 1 m s^{-1} due to a CO_2 increase by a factor of two. Our simulations suggest a bimodal trend favouring no convective updrafts at all or ~~stronger~~ strong updraft mass fluxes (Fig. 7) from 2011 to 2020 compared to 1980 to 1989. ~~Higher maximum values do not occur for the deep convective mass fluxes in our simulations.~~ **?** state that the updraft speed increased the most in the upper troposphere. This is in good agreement with our ~~findings,~~ finding that the deep updraft mass fluxes ~~became~~ get stronger in the upper troposphere from 2011 to 2020 ~~compared to~~ than in the reference time period.

? found in climate projections from 1990 to 2030 that tropical deep convection will reach higher and occur less often. The hindcast simulations from this study confirm these results ~~. Though, in this study, the upraft strength increased for deep convective events in high altitude levels between 30° to 60° North and South in contrast to the results of **?**.~~

~~Furthermore, **?** found~~ for the tropics. Also, **?** obtained a strong correlation ~~of~~ between the deepest convection and the highest tropopause altitudes. ~~However, they assumed based on the diurnal cycles of the tropopause height and the fractional area maximum of convection at lower temperatures as the colder point tropopause that the deep convection causes the colder and higher tropopause and not as supposed in this study the other way around. We cannot conclude with certainty whether there is a causality and which process is the result of the other and therefore, we agree with **?** that further investigations are necessary.~~

5 Conclusions

We ~~applied the submodule CVRANS~~investigated the changes in convective transport due to climate change by applying the submodel CVTRANS, which handles the convective tracer transport in EMAC and can reproduce measured profiles of insoluble tracers (**?**)~~, to investigate the changes in convective transport due to climate change. Thus, we take CVTRANSa step further~~. We made the following adjustments to CVTRANS: (1) ~~by establishing~~ established consistency with the underlying convection scheme (Tiedtke-Nordeng) concerning the turbulent detrainment and entrainment. (2) In addition, the entrained air into the downdraft can be directly ~~detrain in~~ detrained at the same level~~of the downdraft~~. This is comparable to the ~~proceed concerning the updraft~~ procedure for the updraft that was already included in CVTRANS before. (1) and (2) contribute to a more ~~realistic~~ consistent handling of the turbulent mixing associated with convection and give the opportunity to take the effects of turbulent mixing on the redistribution of air masses driven by convection into account. (3) We implemented a new feature, the convective exchange matrix~~. That~~, into CVTRANS. It is similar to the mixing matrix by **?** and opens the path for a new analysis approach for convective transport by directly connecting the convective inflow and outflow levels within EMAC. Thereby, convective transport can be investigated completely disentangled from ~~the~~ other processes.

~~Transient~~ We used the old version of CVTRANS (CVTRANSold), which performs reasonably well in comparison to observations (**?**) in order to contrast it to the new version of CVTRANS with the adaptations for the turbulence (CVTRANSnew). CVTRANSturb is similar to CVTRANSnew but with enhanced turbulence. The latter was used to demonstrate the sensitivity of the convective transport to turbulence; however, too strong turbulent mixing weakens the transport to the upper troposphere to a great extent. Short-cutting the convective transport to such an extent is not beneficial keeping in mind that CVTRANSold performs well, as pointed out by ?. Therefore, CVTRANSnew is used a compromise to keep the results close to the ones of CVTRANSold and to include the consistent turbulent entrainment and detrainment.

The goal of this study was to provide insights into the adjustments of convective tracer transport to global change. Therefore, transient EMAC simulations have been performed using the updated CVTRANS ~~for a 42 year time~~ (CVTRANSnew) for a 42-year period. The convective exchange matrix has been applied to ~~investigate~~ analyse changes in the convective transport due to recorded climate change.

The convective transport reaches higher mainly due to an increase of the tropopause altitude.

~~In the extra-tropics, the~~ The upward transport increased to a wide range of ~~high levels , across which~~ upper tropospheric to lower stratospheric levels in the extra-tropics, where the tropopause height shows substantial variability. However, the changes in the convective transport patterns are~~in general~~ , in general, similar to the tropics. ~~Respectively, less~~ Less material is transported upward from the ~~lower levels to levels between level 26 and 21 which can be~~ boundary layer to levels associated with the free troposphere. This indicates that ~~in total~~ the convective transport is reduced in the extra-tropics in total. The same is the case in the tropics. Globally, this hypothesis is supported by the ~~smaller~~ weaker mean transport from the BL to the UT from 2011 to 2020 in comparison to the reference period. ~~In fact, the~~ The simulations revealed a trend of decreasing occurrence of deep convection. Overall, this leads to less frequent but more penetrative convection, which is in line with the results of **?**.

~~The goal of this study was to provide first insights in the adjustments of convective tracer transport to climate change. On global and zonal scale it becomes emerging that climate change open the path for higher but in total less upward transport of atmospheric tracers by deep convection leading in general to less transport from the BL to the UT. Furthermore, this study opens up new opportunities for the diagnosis of the impacts of convective transport on atmospheric tracers in chemistry climate simulations.~~

The regional trends are accompanied by great uncertainties. The extreme events associated with El Niño and La Niña lead to a large variability within a decade. This makes it hard to identify anthropogenically generated changes on a local ~~scales~~scale. **?** had ~~to deal also with large variability in the historical climate simulations~~ the same issue for the historical time period and determined stronger signals using projections. Therefore, it might be promising to test how the convective transport will ~~change in different climate projectionsbut these test go far beyond the scope of this study~~adapt to climate projections. Moreover, the choice of convection parameterisation is a source of uncertainty ~~which~~ that should be considered. More complex and comprehensive convection parameterisations exist nowadays. ~~A~~ An overview of the developments can be found in **?**. For this reason, we plan to extend this study and investigate the impact of different convection parameterisations in the past and projected climate.

Code and data availability. The Modular Earth Submodel System (MESSy) is being continuously further developed and applied by a consortium of institutions. The usage of MESSy and access to the source code is licensed to all affiliates of institutions who are members of the

MESSy Consortium. Institutions can become a member of the MESSy Consortium by signing the MESSy Memorandum of Understanding. More information can be found on the MESSy Consortium website (http://www.messy-interface.org). The code presented here was developed based on MESSy version 2.55.2 and is available in the developer branch of the model system and therefore also in the next official release. The data and the programme codes for the analysis are available upon request.

Author contributions. AJ and HT designed the study and developed the model code. With contributions from HT, AJ performed the simulations, analysed the data and wrote the paper.

Competing interests. The authors declare that they have no conflict of interest.

Acknowledgements. This research was partially founded by the Deutsche Forschungsgemeinschaft (DFG, German Research Foundation) – TRR 301 – Project-ID 428312742, The Tropopause Region in a Changing Atmosphere. AJ also thank Waves to Weather - the Transregional Collaborative Research Center (SFB/TRR165) for funding until June 2024. We acknowledge Mogon NHR computing system at Johannes Gutenberg-University Mainz and Levante at the German Climate Computing Centre (Deutsches Klimarechenzentrum) for the provided computing time and data disk space. We are grateful for the technical support at Mogon NHR computing system by Andreas Henkel and co-workers. We kindly appreciate Patrick Jöckel for his help concerning the MESSy setup and the code implementation within the MESSy framework. We thank Peter Hoor and Moritz Menken for some discussion. Many thanks to Cornelis Schwenk for his remarks, especially with regard to the ~~the~~ reader's comprehensibility concerning the convective exchange matrix and the idea for Fig.~~S1~~ 2. We are most grateful for the helpful comments leading to an improvement of our manuscript by Wiebke Frey (referee 1) and one anonymous referee. Further, we like to thank our editor Thijs Heus.